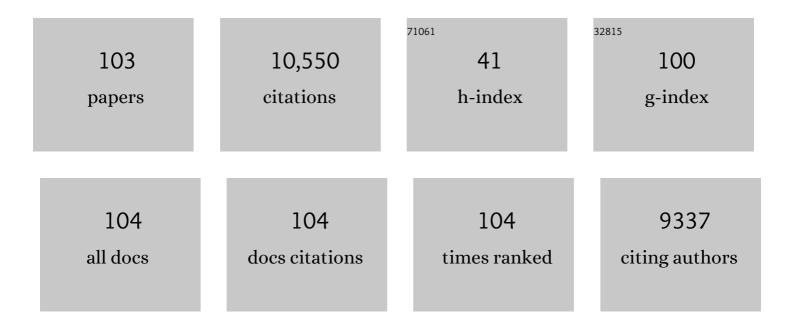
Xiaoyang Zhang

List of Publications by Year in descending order

Source: https://exaly.com/author-pdf/1655956/publications.pdf Version: 2024-02-01



#	Article	IF	CITATIONS
1	First operational BRDF, albedo nadir reflectance products from MODIS. Remote Sensing of Environment, 2002, 83, 135-148.	4.6	2,022
2	Monitoring vegetation phenology using MODIS. Remote Sensing of Environment, 2003, 84, 471-475.	4.6	1,948
3	Climate controls on vegetation phenological patterns in northern mid- and high latitudes inferred from MODIS data. Global Change Biology, 2004, 10, 1133-1145.	4.2	425
4	Land surface phenology from MODIS: Characterization of the Collection 5 global land cover dynamics product. Remote Sensing of Environment, 2010, 114, 1805-1816.	4.6	417
5	Global vegetation phenology from Moderate Resolution Imaging Spectroradiometer (MODIS): Evaluation of global patterns and comparison with in situ measurements. Journal of Geophysical Research, 2006, 111, .	3.3	382
6	Estimating emissions from fires in North America for air quality modeling. Atmospheric Environment, 2006, 40, 3419-3432.	1.9	371
7	Toward mapping crop progress at field scales through fusion of Landsat and MODIS imagery. Remote Sensing of Environment, 2017, 188, 9-25.	4.6	340
8	Remote sensing of the terrestrial carbon cycle: A review of advances over 50 years. Remote Sensing of Environment, 2019, 233, 111383.	4.6	276
9	Diverse responses of vegetation phenology to a warming climate. Geophysical Research Letters, 2007, 34, .	1.5	235
10	The footprint of urban climates on vegetation phenology. Geophysical Research Letters, 2004, 31, n/a-n/a.	1.5	234
11	Biomass burning impact on PM _{2.5} over the southeastern US during 2007: integrating chemically speciated FRM filter measurements, MODIS fire counts and PMF analysis. Atmospheric Chemistry and Physics, 2010, 10, 6839-6853.	1.9	209
12	Monitoring the response of vegetation phenology to precipitation in Africa by coupling MODIS and TRMM instruments. Journal of Geophysical Research, 2005, 110, .	3.3	186
13	Exploration of scaling effects on coarse resolution land surface phenology. Remote Sensing of Environment, 2017, 190, 318-330.	4.6	149
14	Sensitivity of vegetation phenology detection to the temporal resolution of satellite data. International Journal of Remote Sensing, 2009, 30, 2061-2074.	1.3	142
15	Reconstruction of a complete global time series of daily vegetation index trajectory from long-term AVHRR data. Remote Sensing of Environment, 2015, 156, 457-472.	4.6	133
16	Using data from Landsat, MODIS, VIIRS and PhenoCams to monitor the phenology of California oak/grass savanna and open grassland across spatial scales. Agricultural and Forest Meteorology, 2017, 237-238, 311-325.	1.9	131
17	Satellite detection of cumulative and lagged effects of drought on autumn leaf senescence over the Northern Hemisphere. Global Change Biology, 2019, 25, 2174-2188.	4.2	126
18	Evaluation of land surface phenology from VIIRS data using time series of PhenoCam imagery. Agricultural and Forest Meteorology, 2018, 256-257, 137-149.	1.9	125

#	Article	IF	CITATIONS
19	Generation and evaluation of the VIIRS land surface phenology product. Remote Sensing of Environment, 2018, 216, 212-229.	4.6	110
20	Spring green-up phenology products derived from MODIS NDVI and EVI: Intercomparison, interpretation and validation using National Phenology Network and AmeriFlux observations. Ecological Indicators, 2017, 77, 323-336.	2.6	97
21	Evaluation of the VIIRS BRDF, Albedo and NBAR products suite and an assessment of continuity with the long term MODIS record. Remote Sensing of Environment, 2017, 201, 256-274.	4.6	89
22	Monitoring fall foliage coloration dynamics using time-series satellite data. Remote Sensing of Environment, 2011, 115, 382-391.	4.6	84
23	Interannual variations and trends in global land surface phenology derived from enhanced vegetation index during 1982–2010. International Journal of Biometeorology, 2014, 58, 547-564.	1.3	81
24	Mapping Crop Phenology in Near Real-Time Using Satellite Remote Sensing: Challenges and Opportunities. Journal of Remote Sensing, 2021, 2021, .	3.2	77
25	Monitoring interannual variation in global crop yield using long-term AVHRR and MODIS observations. ISPRS Journal of Photogrammetry and Remote Sensing, 2016, 114, 191-205.	4.9	75
26	Nearâ€realâ€time global biomass burning emissions product from geostationary satellite constellation. Journal of Geophysical Research, 2012, 117, .	3.3	72
27	Near real time monitoring of biomass burning particulate emissions (PM2.5) across contiguous United States using multiple satellite instruments. Atmospheric Environment, 2008, 42, 6959-6972.	1.9	69
28	Comparison of Fire Radiative Power Estimates From VIIRS and MODIS Observations. Journal of Geophysical Research D: Atmospheres, 2018, 123, 4545-4563.	1.2	69
29	Development and evaluation of a new algorithm for detecting 30Âm land surface phenology from VIIRS and HLS time series. ISPRS Journal of Photogrammetry and Remote Sensing, 2020, 161, 37-51.	4.9	69
30	Drought-induced vegetation stress in southwestern North America. Environmental Research Letters, 2010, 5, 024008.	2.2	68
31	Temporal and spatial variability in biomass burned areas across the USA derived from the GOES fire product. Remote Sensing of Environment, 2008, 112, 2886-2897.	4.6	64
32	Estimation of biomass-burning emissions by fusing the fire radiative power retrievals from polar-orbiting and geostationary satellites across the conterminous United States. Atmospheric Environment, 2019, 211, 274-287.	1.9	64
33	Intercomparison and evaluation of spring phenology products using National Phenology Network and AmeriFlux observations in the contiguous United States. Agricultural and Forest Meteorology, 2017, 242, 33-46.	1.9	58
34	Scaling effects on spring phenology detections from MODIS data at multiple spatial resolutions over the contiguous United States. ISPRS Journal of Photogrammetry and Remote Sensing, 2017, 132, 185-198.	4.9	58
35	Long-term continuity in land surface phenology measurements: A comparative assessment of the MODIS land cover dynamics and VIIRS land surface phenology products. Remote Sensing of Environment, 2019, 226, 74-92.	4.6	53
36	Sensitivity of mesoscale modeling of smoke direct radiative effect to the emission inventory: a case study in northern sub-Saharan African region. Environmental Research Letters, 2014, 9, 075002.	2.2	51

#	Article	IF	CITATIONS
37	Urbanization imprint on land surface phenology: The urban–rural gradient analysis for Chinese cities. Global Change Biology, 2021, 27, 2895-2904.	4.2	51
38	Monitoring land surface albedo and vegetation dynamics using high spatial and temporal resolution synthetic time series from Landsat and the MODIS BRDF/NBAR/albedo product. International Journal of Applied Earth Observation and Geoinformation, 2017, 59, 104-117.	1.4	49
39	A preliminary evaluation of GOES-16 active fire product using Landsat-8 and VIIRS active fire data, and ground-based prescribed fire records. Remote Sensing of Environment, 2020, 237, 111600.	4.6	45
40	Comparisons of global land surface seasonality and phenology derived from AVHRR, MODIS, and VIIRS data. Journal of Geophysical Research G: Biogeosciences, 2017, 122, 1506-1525.	1.3	44
41	Daily MODIS 500 m reflectance anisotropy direct broadcast (DB) products for monitoring vegetation phenology dynamics. International Journal of Remote Sensing, 2013, 34, 5997-6016.	1.3	42
42	Widespread decline in winds delayed autumn foliar senescence over high latitudes. Proceedings of the United States of America, 2021, 118, .	3.3	41
43	The Influences of Drought and Land-Cover Conversion on Inter-Annual Variation of NPP in the Three-North Shelterbelt Program Zone of China Based on MODIS Data. PLoS ONE, 2016, 11, e0158173.	1.1	41
44	Precipitation and Minimum Temperature are Primary Climatic Controls of Alpine Grassland Autumn Phenology on the Qinghai-Tibet Plateau. Remote Sensing, 2020, 12, 431.	1.8	41
45	Impacts of land cover and land use change on long-term trend of land surface phenology: a case study in agricultural ecosystems. Environmental Research Letters, 2019, 14, 044020.	2.2	39
46	Interannual variation in biomass burning and fire seasonality derived from geostationary satellite data across the contiguous United States from 1995 to 2011. Journal of Geophysical Research G: Biogeosciences, 2014, 119, 1147-1162.	1.3	38
47	A Cross Comparison of Spatiotemporally Enhanced Springtime Phenological Measurements From Satellites and Ground in a Northern U.S. Mixed Forest. IEEE Transactions on Geoscience and Remote Sensing, 2014, 52, 7513-7526.	2.7	35
48	Investigation of land surface phenology detections in shrublands using multiple scale satellite data. Remote Sensing of Environment, 2021, 252, 112133.	4.6	35
49	Reconstruction of Daily 30 m Data from HJ CCD, GF-1 WFV, Landsat, and MODIS Data for Crop Monitoring. Remote Sensing, 2015, 7, 16293-16314.	1.8	33
50	A Comparison of Tropical Rainforest Phenology Retrieved From Geostationary (SEVIRI) and Polar-Orbiting (MODIS) Sensors Across the Congo Basin. IEEE Transactions on Geoscience and Remote Sensing, 2016, 54, 4867-4881.	2.7	32
51	Real-Time Monitoring of Crop Phenology in the Midwestern United States Using VIIRS Observations. Remote Sensing, 2018, 10, 1540.	1.8	32
52	Estimation of Biomass Burned Areas Using Multiple-Satellite-Observed Active Fires. IEEE Transactions on Geoscience and Remote Sensing, 2011, 49, 4469-4482.	2.7	31
53	Prototype for monitoring and forecasting fall foliage coloration in real time from satellite data. Agricultural and Forest Meteorology, 2012, 158-159, 21-29.	1.9	31
54	Evaluating land surface phenology from the Advanced Himawari Imager using observations from MODIS and the Phenological Eyes Network. International Journal of Applied Earth Observation and Geoinformation, 2019, 79, 71-83.	1.4	29

#	Article	IF	CITATIONS
55	Investigation of the Fire Radiative Energy Biomass Combustion Coefficient: A Comparison of Polar and Geostationary Satellite Retrievals Over the Conterminous United States. Journal of Geophysical Research G: Biogeosciences, 2018, 123, 722-739.	1.3	28
56	A new algorithm for the estimation of leaf unfolding date using MODIS data over China's terrestrial ecosystems. ISPRS Journal of Photogrammetry and Remote Sensing, 2019, 149, 77-90.	4.9	28
57	Investigation of wildfire impacts on land surface phenology from MODIS time series in the western US forests. ISPRS Journal of Photogrammetry and Remote Sensing, 2020, 159, 281-295.	4.9	28
58	Dominance of Wildfires Impact on Air Quality Exceedances During the 2020 Recordâ€Breaking Wildfire Season in the United States. Geophysical Research Letters, 2021, 48, e2021GL094908.	1.5	28
59	Real-time and short-term predictions of spring phenology in North America from VIIRS data. Remote Sensing of Environment, 2017, 194, 89-99.	4.6	26
60	Burned Area Comparisons Between Prescribed Burning Permits in Southeastern United States and Two Satelliteâ€Đerived Products. Journal of Geophysical Research D: Atmospheres, 2018, 123, 4746-4757.	1.2	25
61	How Does Scale Effect Influence Spring Vegetation Phenology Estimated from Satellite-Derived Vegetation Indexes?. Remote Sensing, 2019, 11, 2137.	1.8	25
62	Interannual variations in spring phenology and their response to climate change across the Tibetan Plateau from 1982 to 2013. International Journal of Biometeorology, 2016, 60, 1563-1575.	1.3	22
63	An Exploration of Terrain Effects on Land Surface Phenology across the Qinghai–Tibet Plateau Using Landsat ETM+ and OLI Data. Remote Sensing, 2018, 10, 1069.	1.8	22
64	Impacts of wildfires on interannual trends in land surface phenology: an investigation of the Hayman Fire. Environmental Research Letters, 2017, 12, 054008.	2.2	21
65	Scaling up spring phenology derived from remote sensing images. Agricultural and Forest Meteorology, 2018, 256-257, 207-219.	1.9	21
66	Ensemble PM _{2.5} Forecasting During the 2018 Camp Fire Event Using the HYSPLIT Transport and Dispersion Model. Journal of Geophysical Research D: Atmospheres, 2020, 125, e2020JD032768.	1.2	21
67	Effects of temperature variability and extremes on spring phenology across theÂcontiguous United States from 1982 to 2016. Scientific Reports, 2020, 10, 17952.	1.6	21
68	Mapping corn and soybean phenometrics at field scales over the United States Corn Belt by fusing time series of Landsat 8 and Sentinel-2 data with VIIRS data. ISPRS Journal of Photogrammetry and Remote Sensing, 2022, 186, 55-69.	4.9	21
69	The implementation of NEMS GFS Aerosol Component (NGAC) Version 2.0 for global multispecies forecasting at NOAA/NCEP – PartÂ1: Model descriptions. Geoscientific Model Development, 2018, 11, 2315-2332.	1.3	20
70	Detecting spatiotemporal changes of peak foliage coloration in deciduous and mixedforests across the Central and Eastern United States. Environmental Research Letters, 2017, 12, 024013.	2.2	19
71	Impacts of Thermal Time on Land Surface Phenology in Urban Areas. Remote Sensing, 2017, 9, 499.	1.8	19
72	Biomass Burning in Africa: An Investigation of Fire Radiative Power Missed by MODIS Using the 375 m VIIRS Active Fire Product. Remote Sensing, 2020, 12, 1561.	1.8	19

#	Article	IF	CITATIONS
73	Use of hourly Geostationary Operational Environmental Satellite (GOES) fire emissions in a Community Multiscale Air Quality (CMAQ) model for improving surface particulate matter predictions. Journal of Geophysical Research, 2011, 116, .	3.3	17
74	Estimating the Aboveground Biomass for Planted Forests Based on Stand Age and Environmental Variables. Remote Sensing, 2019, 11, 2270.	1.8	17
75	Detection of Fire Smoke Plumes Based on Aerosol Scattering Using VIIRS Data over Global Fire-Prone Regions. Remote Sensing, 2021, 13, 196.	1.8	15
76	Eutrophication monitoring of lakes in Wuhan based on Sentinel-2 data. GIScience and Remote Sensing, 2021, 58, 776-798.	2.4	15
77	An evaluation of advanced baseline imager fire radiative power based wildfire emissions using carbon monoxide observed by the Tropospheric Monitoring Instrument across the conterminous United States. Environmental Research Letters, 2020, 15, 094049.	2.2	15
78	Characterizing Land Cover Impacts on the Responses of Land Surface Phenology to the Rainy Season in the Congo Basin. Remote Sensing, 2017, 9, 461.	1.8	14
79	Hybrid phenology matching model for robust crop phenological retrieval. ISPRS Journal of Photogrammetry and Remote Sensing, 2021, 181, 308-326.	4.9	14
80	Quantifying Carbon Monoxide Emissions on the Scale of Large Wildfires. Geophysical Research Letters, 2022, 49, .	1.5	14
81	Crop Growth Condition Assessment at County Scale Based on Heat-Aligned Growth Stages. Remote Sensing, 2019, 11, 2439.	1.8	13
82	Satellite-observed decrease in the sensitivity of spring phenology to climate change under high nitrogen deposition. Environmental Research Letters, 2020, 15, 094055.	2.2	13
83	Fusing Geostationary Satellite Observations with Harmonized Landsat-8 and Sentinel-2 Time Series for Monitoring Field-Scale Land Surface Phenology. Remote Sensing, 2021, 13, 4465.	1.8	13
84	Investigating Smoke Aerosol Emission Coefficients Using MODIS Active Fire and Aerosol Products: A Case Study in the CONUS and Indonesia. Journal of Geophysical Research G: Biogeosciences, 2019, 124, 1413-1429.	1.3	12
85	Characteristics of Greening along Altitudinal Gradients on the Qinghai–Tibet Plateau Based on Time-Series Landsat Images. Remote Sensing, 2022, 14, 2408.	1.8	11
86	Mapping Temperate Vegetation Climate Adaptation Variability Using Normalized Land Surface Phenology. Climate, 2016, 4, 24.	1.2	10
87	Land cover composition, climate, and topography drive land surface phenology in a recently burned landscape: An application of machine learning in phenological modeling. Agricultural and Forest Meteorology, 2021, 304-305, 108432.	1.9	10
88	Incorporating water availability into autumn phenological model improved China's terrestrial gross primary productivity (GPP) simulation. Environmental Research Letters, 2021, 16, 094012.	2.2	10
89	Highly anomalous fire emissions from the 2019–2020 Australian bushfires. Environmental Research Communications, 2021, 3, 105005.	0.9	10
90	Spatiotemporal characteristics of white mold and impacts on yield in soybean fields in South Dakota. Geo-Spatial Information Science, 2020, 23, 182-193.	2.4	9

#	Article	IF	CITATIONS
91	Exploring discrepancies between in situ phenology and remotely derived phenometrics at <scp>NEON</scp> sites. Ecosphere, 2022, 13, .	1.0	9
92	Trends in land surface phenology across the conterminous United States (1982â€2016) analyzed by NEON domains. Ecological Applications, 2021, 31, e02323.	1.8	8
93	Evaluating a spatiotemporal shape-matching model for the generation of synthetic high spatiotemporal resolution time series of multiple satellite data. International Journal of Applied Earth Observation and Geoinformation, 2021, 104, 102545.	1.4	8
94	Pronounced increases in nitrogen emissions and deposition due to the historic 2020 wildfires in the western U.S Science of the Total Environment, 2022, 839, 156130.	3.9	6
95	Drainage canal impacts on smoke aerosol emissions for Indonesian peatland and non-peatland fires. Environmental Research Letters, 2021, 16, 095008.	2.2	5
96	Increasing Interspecific Difference of Alpine Herb Phenology on the Eastern Qinghai-Tibet Plateau. Frontiers in Plant Science, 2022, 13, 844971.	1.7	5
97	Exploration of global spatiotemporal changes of fall foliage coloration in deciduous forests and shrubs using the VIIRS land surface phenology product. Science of Remote Sensing, 2021, 4, 100030.	2.2	4
98	Land Surface Phenology: Climate Data Record and Real-Time Monitoring. , 2018, , 35-52.		3
99	Mapping and Quantifying White Mold in Soybean across South Dakota Using Landsat Images. Journal of Geographic Information System, 2019, 11, 331-346.	0.3	3
100	Using remote sensing to monitor the spring phenology of Acadia National Park across elevational gradients. Ecosphere, 2021, 12, .	1.0	2
101	Development of Global Land Surface Phenology Product from Time Series of VIIRS Observations. , 2020, , .		1
102	Spatial Difference between Temperature and Snowfall Driven Spring Phenology of Alpine Grassland Land Surface Based on Process-Based Modeling on the Qinghai–Tibet Plateau. Remote Sensing, 2022, 14, 1273.	1.8	1
103	Soybean EOS Spatiotemporal Characteristics and Their Climate Drivers in Global Major Regions. Remote Sensing, 2022, 14, 1867.	1.8	1